LASER GENERATED STRESS WAVES: THEIR CHARACTERISTICS AND THEIR EFFECTS TO MATERIALS

B. P. Fairand and A. H. Clauer
Battelle Memorial Institute, 505 King Avenue, Columbus, Ohio 43201

ABSTRACT

When the energy from a powerful pulsed laser is trained on the surface of an absorbent material, a high-amplitude stress wave is generated. If the surface is covered with a material which is transparent to the incident laser light, peak pressure environments are significantly enhanced compared to free surface conditions. Experimental pressure measurements using piezoelectric pressure transducers have demonstrated that peak pressures up to approximately 10 GPa can be generated in this manner. The rise time of these pressure waves, which is controlled by the temperature of the laser heated absorbent material, approximates the shape of the incident laser pulse. The decay time of the pressure waves is slower than the laser pulse because it is governed by the rate at which work is done on surrounding materials and the rate at which heat is conducted out of the heated vapor into colder adjacent materials. Theoretical calculations of the pressure environments using a one-dimensional radiation hydrodynamic computer code are in good agreement with the experimental measurements.

The stress wave propagates into the material and modifies the material's substructure and properties in a way similar to shock waves generated by other means. This process has been successfully used to increase the strength and hardness of several aluminum alloys, titanium, and the hardness of stainless steel. The yield strength of the heat-affected zones in welded aluminum structures has been increased to values up to the strength of the parent material. Recent studies have demonstrated that laser shock processing can also be used to improve the fatigue life in an aluminum alloy.

INTRODUCTION

The potential of using pulsed lasers to generate high intensity stress waves in materials was first recognized and explored by the early nineteen sixties.[1,2] Later work established that a major enhancement in the amplitude of the laser generated stress waves occurred if the absorbent surface was covered with a material transparent to the incident laser light.[3-8] Stress waves generated under these conditions were found to be sufficiently intense to plastically deform metals and alloys even when the experiments were conducted in a gas environment such as air at standard conditions.[9-11] The ability to generate high intensity pressure environments in materials without imposing the constraint of conducting the experiments in vacuum stimulated interest in using these laser induced pressure waves to alter the properties of materials in a manner similar to high explosive and flyer plate shock deformation of metals and alloys. The laser also offered attractive characteristics as a source of high intensity pressure environments which provided added incentive for investigating the properties and applications of laser generated stress waves.

This paper examines the types of high amplitude pressure environments one can generate with a pulsed laser and defines important parameters governing the interaction mechanisms and their impact on the resultant pressures. This analysis is confined to a pulsed neodymium-glass laser because it was the experimental facility used in essentially all of our investigations; however, other lasers with wave-lengths ranging from the infrared to the visible and near ultra-violet have the potential of producing similar environments.

The effects of these stress waves to the surface and in-depth-properties of materials also is investigated in this paper. These effects range from increasing the surface hardness to improvements in yield strength and increases in the fatigue life of other metals.

PROPERTIES OF LASER GENERATED STRESS WAVES

An understanding of the effects to material properties by the laser induced stress waves first requires a quantitative description of the pressure environments generated at the surface of the material and how changes in the laser parameters and surface conditions of the target affect these pressure environments. These properties of laser generated stress waves are described in this section of the paper. A second important consideration which is required to complete our understanding of the effects of these stress waves to materials is the propagation characteristics of the stress waves and modifications of the in-depth stress fields introduced by physical and geometrical boundaries. Work published in this area for laser induced stress wave environments and flyer plate experiments clearly demonstrate that boundaries affect the resultant in-depth stress wave environments and modes of deformation.[12,13] Work is presently underway to explore in detail the in-depth properties of laser induced stress waves and the material deformation introduced by these environments. This work will be reported at a later date.

EXPERIMENTAL AND THEORETICAL ANALYSIS OF SOURCE PRESSURE ENVIRONMENTS

Most of our laser generated stress wave studies utilized a high power CGE VD-640 Q-switched neodymium-glass laser, which consists of an oscillator followed by six amplifier stages. This system is able to emit pulses with full widths at one-half maximum (FWHM) ranging from 1 nanosecond to about 100 nanoseconds and energies up to 500 J. In addition to the CGE laser, some work was conducted with a

5 joule A.O. Model 30 Q-switched neodymium-glass laser which has pulse width (FWHM) of approximately 40 nanoseconds. The shapes of the laser pulses emitted by these systems were measured with photodiode detectors whose outputs were fed to fast oscilloscopes.

Carbon calorimeters were used to monitor the output energies of the two laser systems. The procedure was to measure the energy arriving at the experimental site and then normalize this energy to an on-line calorimeter which detected a small fraction of the incident beam emanating from a beam splitter.

Dielectric mirrors were used to direct the laser radiation to the target material and simple convex convergent lenses were used to focus the laser radiation to the desired spot size.

The pressures were measured with commercially available X-cut quartz crystal transducers of a shorted guard-ring design. Metal targets to measure the pressure environments produced on metallic surfaces were prepared by vacuum depositing 3-μm-thick films directly onto the front electrode surface of the quartz transducers. In some of the pressure measurements, a layer of black paint was sprayed onto the metal surface or directly onto the transducer electrode before application of the transparent overlay material. Transparent materials with widely differing acoustic impedances, e.g. water, plastic, and glass (quartz) were used to evaluate the effect of this parameter on the amplitude and time history of the stress waves. Metal targets with different thermal properties also were investigated to determine the effect of these parameters on the pressure environments. The experimental pressure measurements were compared to theoretical predictions obtained from a one-dimensional code called LILA. This code which is based on the method of finite differences was used to simulate the thermal and hydrodynamic response of materials irradiated by a laser beam. A description of the models contained in this code is presented in another publication.[14] Basically, absorption of laser light in metal targets is first treated by classical interaction of electromagnetic radiation with a metallic conductor and then in the heated plasma, the absorptance is handled via an inverse Bremsstrahlung process. An analytical equation of state is used to describe the behavior of the metal by a superposition of terms including zero temperature behavior, thermal motion of heavy particles, and the thermal excitation and ionization of electrons. Thermal transport processes include radiation diffusion and conduction by the metal atoms and ionized electrons in the plasma.

RESULTS OF ANALYSIS

The shape and amplitude of the resultant stress wave depends on the temperature history of the heated vapor. This in turn depends on the laser power density at the interaction surface and the laser energy deposition time. The laser energy must be deposited in a relatively short time to avoid the diffusion of energy away from the interaction zone and the effect of hydrodynamic processes, both of which reduce the amplitude of the stress wave. The thermal conductivity and heat of vaporization of the absorbent material can also affect the stress wave environment, particularly as one goes to lower power densities.

The measured and predicted peak pressure environments generated in different target materials covered with different transparent overlays is shown in Figure 1 as a function of the incident laser power density, e.g. energy per unit area, divided by the width of the laser pulse. The peak pressures calculated by the LILA code, which are shown as curves through the data, are in good agreement with the experimental data. As seen from Figure 1, the use of different target absorbers has little effect on peak pressure once the incident laser power densities are increased above 1-2 x 10^9 W/cm^2. At these higher laser power densities, calculations predict most of the absorbed energy initially goes into heating of the vapor. For this reason, the shape of the stress wave closely follows the shape of the laser pulse until the laser pulse begins to decay The decay time of the stress waves is much slower because it is governed by the rate at which work is done on surrounding materials and the rate at which heat is conducted out of the vapor into the colder adjacent materials. Experimental measurements of pressure confirm this type of behavior. This is illustrated in Figure 2 which compares the measured time history of the laser pulse with the measured pressure pulse for the case of a transparent water overlay on aluminum and quartz over aluminum.

When laser power densities are decreased below approximately 1 x 10^9 W/cm^2, thermal properties of the absorbent material begin to have a significant effect on the pressure environments. This is the reason the two peak pressure curves shown in Figure 1 for quartz overlays begin to diverge as the value of the laser power density approaches 1 x 10^9 W/cm^2. It has been determined that materials with low thermal conductivities tend to confine the absorbed energy to the interaction zone for longer times, thus maintaining the high temperatures needed to generate high amplitude pressures. With low heat of vaporization material, more energy is available for heating purposes and less energy is lost to internal energy of the phase change.

Figure 3 shows the effect to the pressure environments and temperatures in the interaction zone from changing the thermal properties of the absorber. These predicted curves demonstrate that zinc with its lower thermal conductivity and heat of vaporization is able to generate higher amplitude and longer duration pressure pulses than aluminum given the same incident laser environment.

The change in pressure resulting from the use of different transparent overlays also is illustrated in Figure 1. The controlling factor in this case is the acoustic impedance of the overlay material. Water has an acoustic impedance about 1/10 that of quartz, which is the reason the pressures generated with water overlays are lower than quartz. It is important to note, however, that water still provides an effective method of generating high amplitude stress waves needed to shock process materials. From a practical standpoint, when using laser shocking as a materials processing method, liquids such as water have obvious advantages over solid overlays.

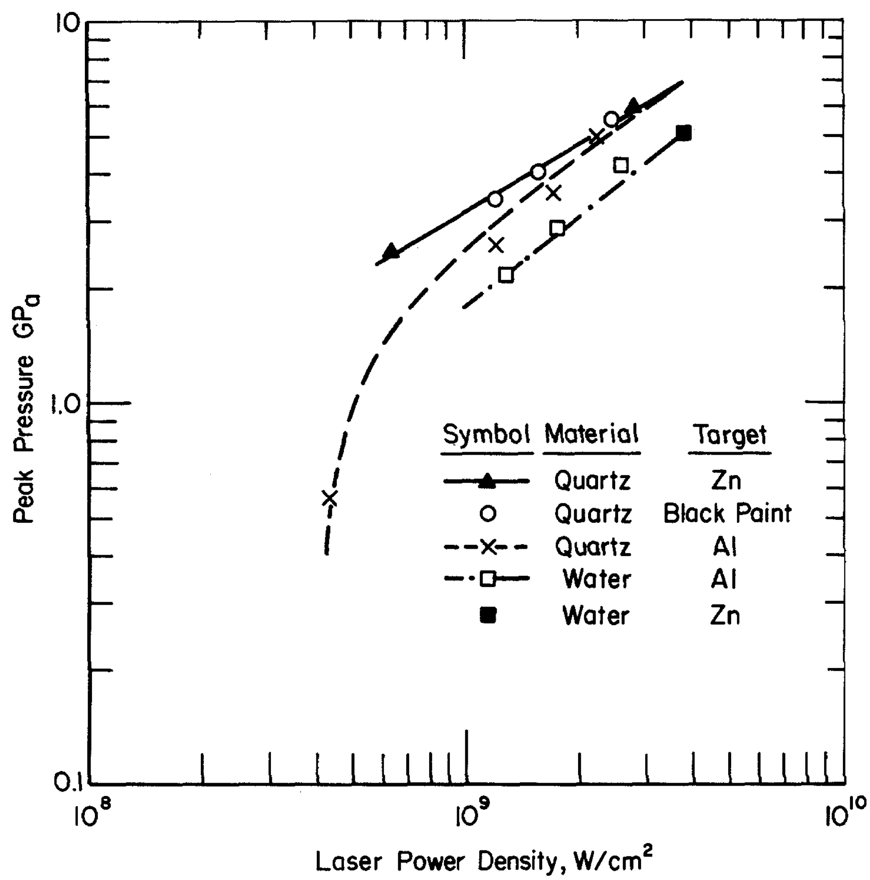

Fig. 1. Comparison of predicted and measured peak pressures generated in different target films confined by quartz or water overlays.

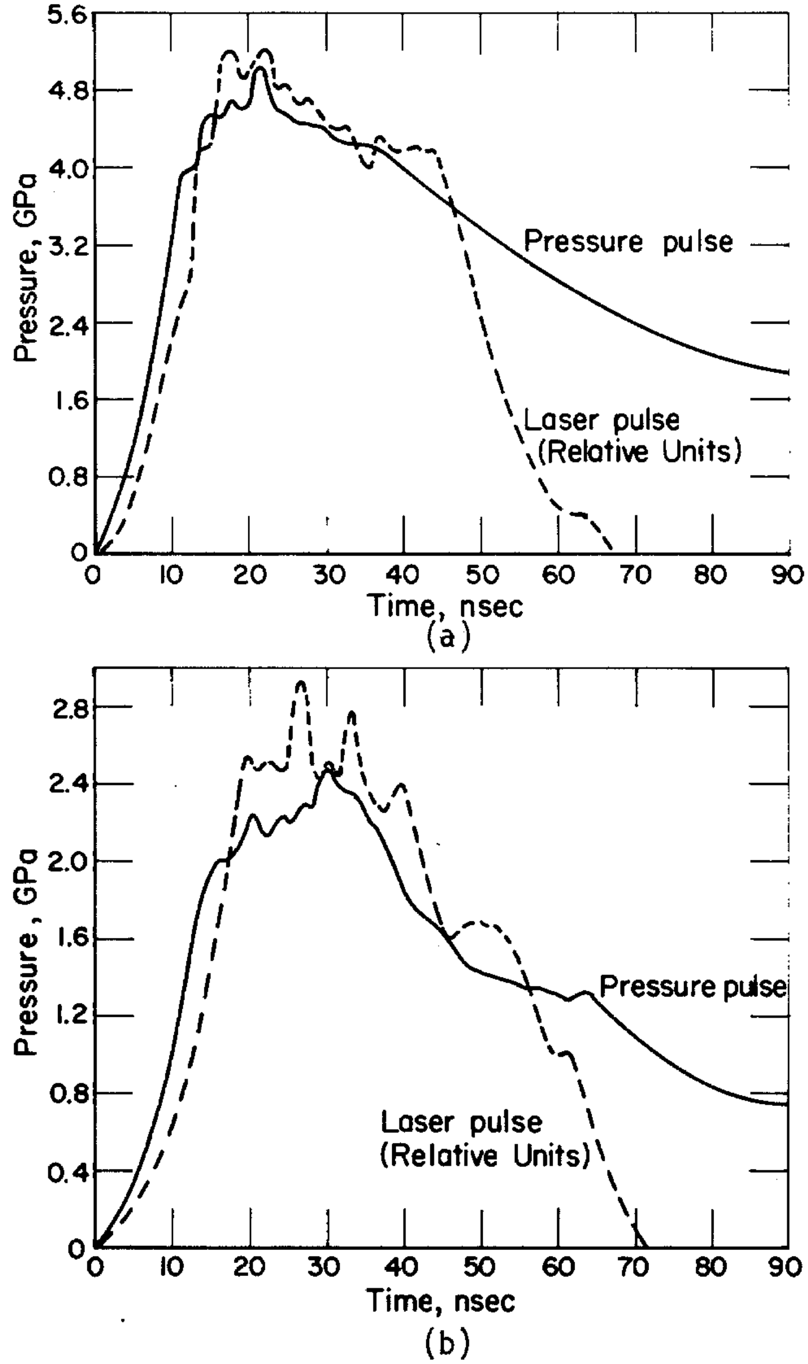

Fig. 2. Comparison of measured laser pulses with pressure pulses. (a) Quartz overlay. (b) Water overlay.

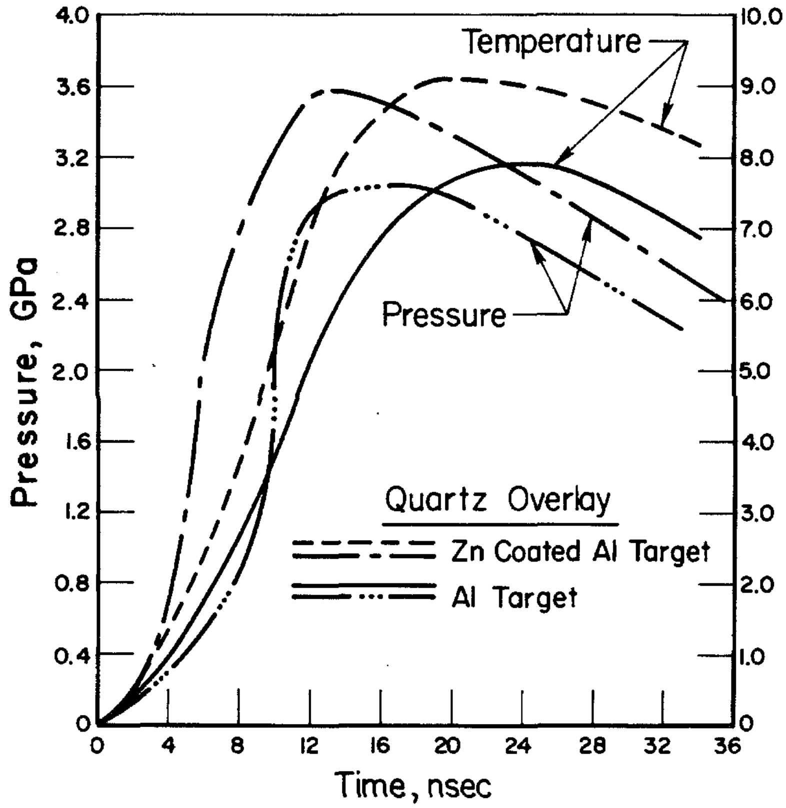

Fig. 3. Comparison of temperature and pressure histories for an aluminum and zinc target.

MATERIAL EFFECTS

The response of materials to laser shocking was first investigated by looking at changes in hardness and tensile properties of alloys and studying the modified microstructures.[9] In some cases, these results could be compared to the large body of information generated from high explosive and flyer plate shocking of materials. Later work was directed more toward possible applications of the laser shock process. For example, increases in the strength properties of welded structures were investigated and other properties such as fatigue and corrosion resistance were examined.

Iron base alloys, several aluminum alloys and a titanium alloy have been included in our studies. The iron alloys consisted of stainless steel and an Fe 3wt% Si alloy which was selected for research purposes because it can be etch-pitted for visual examination of the laser-shock-induced strain field. In the case of aluminum, both non-heat-treatable and heat-treatable alloys in the peak and overaged conditions have been laser shocked. Results of this work are discussed in the following sections.

ALUMINUM ALLOYS

The first alloys to be laser shocked were a 7075 T73 aluminum in the overaged condition and a 7075 T6 aluminum in the peak aged condition.[9] Based on these experiments, it was determined that the mechanical properties, e.g., strength and hardness, of the overaged alloy responded favorably to the laser shock treatment. For example, in 7075 T73, tensile tests showed that the 0.2% offset yield strength was increased as much as 30% over unshocked values and the ultimate strength was increased more than 10%. Laser shocking of the peak aged alloy under similar laser conditions resulted in little change in the mechanical properties. These changes in the mechanical properties were interpreted in terms of the microstructural changes induced by laser shocking. Transmission electron micrographs of the unshocked and shocked microstructures of these two alloys are shown in Figure 4. As seen from this figure, the shocking process introduced a very dense tangled dislocation substructure. These shocked microstructures were similar to those produced by high explosive shocking.[15] The lack of shock strengthening in the peak aged condition is understandable because strengthening due to fine precipitates present in the unshocked substructure mitigates any possible strength contribution due to the shock-induced dislocation substructure. Later work with peak aged and underaged 2024 aluminum alloys exhibited the same type of behavior. The surface hardness of an underaged 2024 T3 was increased by more than 20% over its unshocked value which was approximately the hardness increase caused by heavy cold working of the alloy. The peak aged 2024 T8 alloy, on the other hand, showed little change in surface hardness. Recent work at higher incident power densities and pressures shows that even the peak aged alloys will respond favorably to the laser shock treatment. The higher pressure requirements for improving the properties of peak aged alloys are due to the higher yield strength and lower strain hardening rates in these alloys. These results are consistent with flyer plate shocking of the same alloys.[16]

There are several possible applications where laser shock treatment of aluminum alloys may offer a new and important processing procedure. One example might be the in situ treatment of "soft" weld zones. In many welded aluminum structures, the weld and its adjacent heat affected zone (HAZ) are a region of weakness having a lower strength than the rest of the structure. The strength of this region can be increased by a post-weld heat treatment or by mechanical working, such as rolling the weld bead or explosive shocking. These approaches, however, are often either not practicable or are undesirable. Laser shocking offers an alternative technique for increasing the strength properties of weld zones without introducing the undesirable aspects of other post weld treatment processes. To test the laser's ability to shock process weld zones, tensile specimens were cut from welded plates of 5086 H32 and 6061 T6 aluminum and laser shocked. The 5086 H32 aluminum is a solid-solution strengthened alloy and 6061 T6 is a peak aged age-hardenable alloy. Tensile tests were run on shocked and unshocked specimens. Results of these tests are shown in Figure 5. As seen in this figure, after laser shocking, the tensile yield strength of 5086 H32 was raised to the bulk value and the strength of 6061 T6 was raised midway between the welded and bulk levels. The change in microstructure which is responsible for this change in strength properties is illustrated in Figure 6. The shocked microstructure shows heavy dislocation ranges typical of cold working.

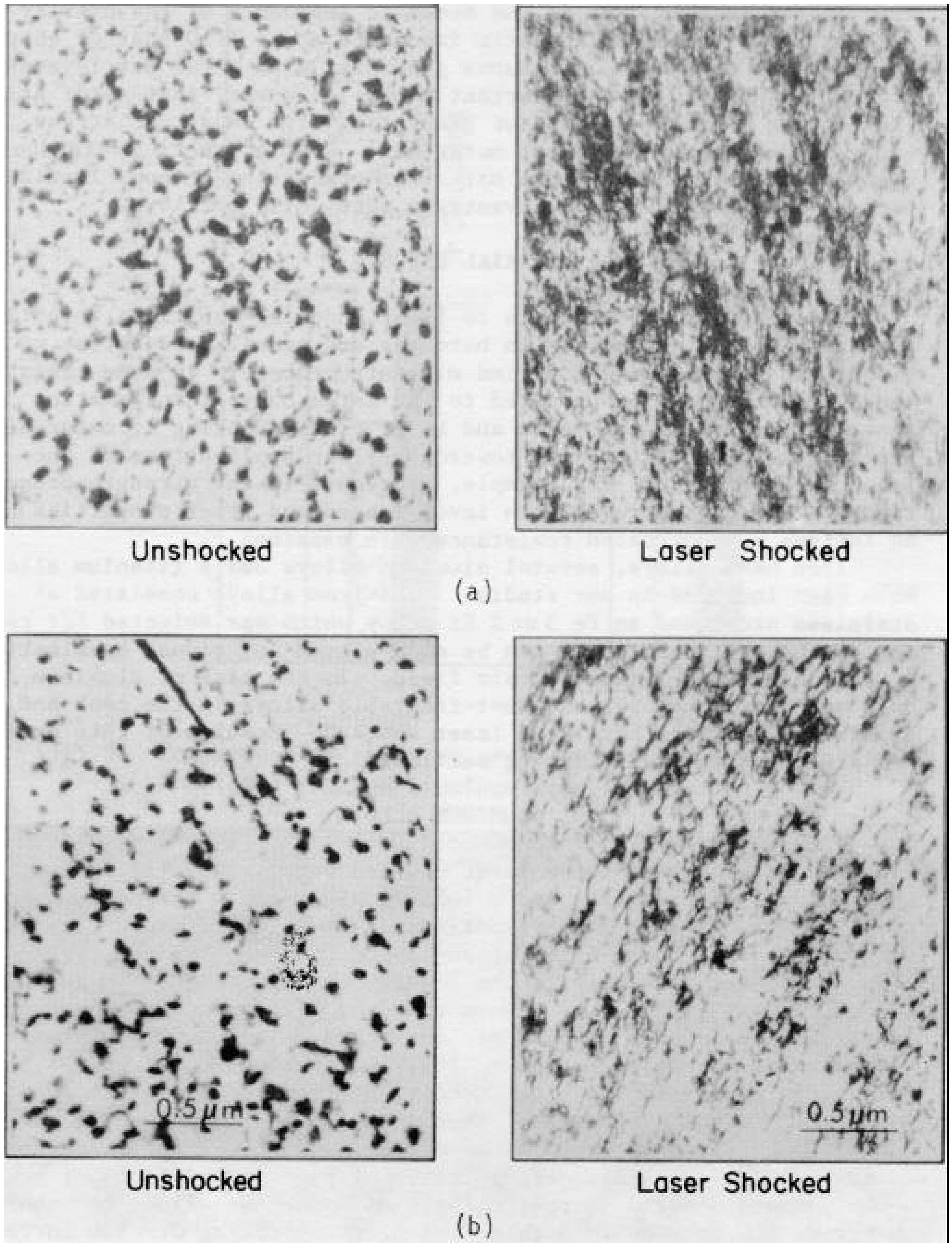

Fig. 4. Microstructures of unshocked and shocked aluminum alloys.
(a) 7075 T73 aluminum alloy.
(b) 7075 T6 aluminum alloy.

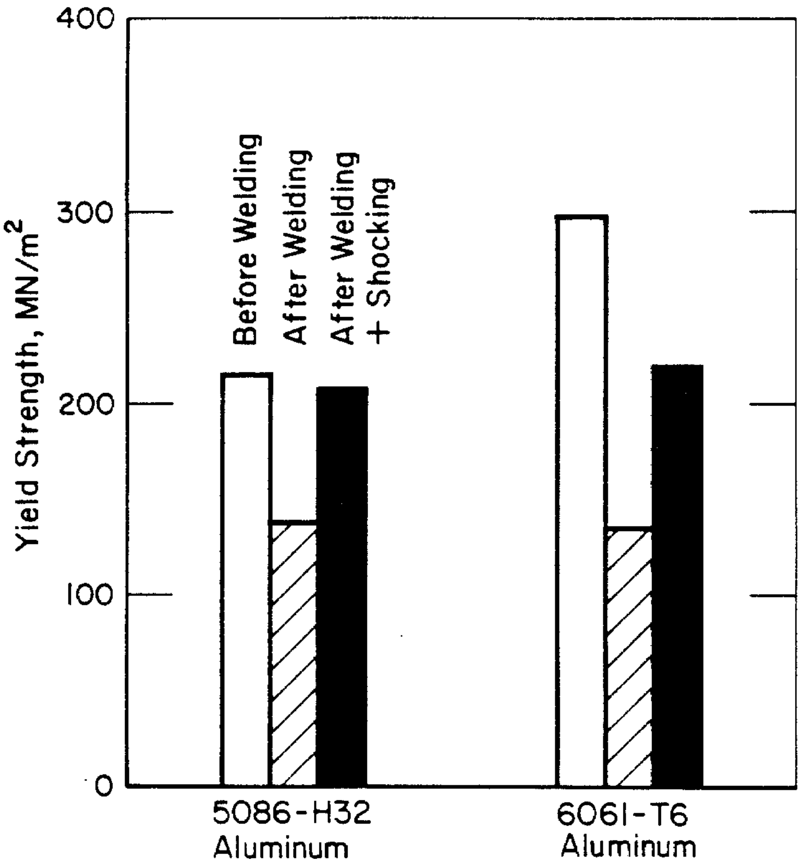

Fig. 5. Comparison of the 0.2% offset yield strength of welded and laser shocked aluminum alloys.

Fig. 6. Comparison of the microstructures of welded and laser shocked aluminum alloys. (a) Initial condition. (b) After welding. (c) After laser shocking.

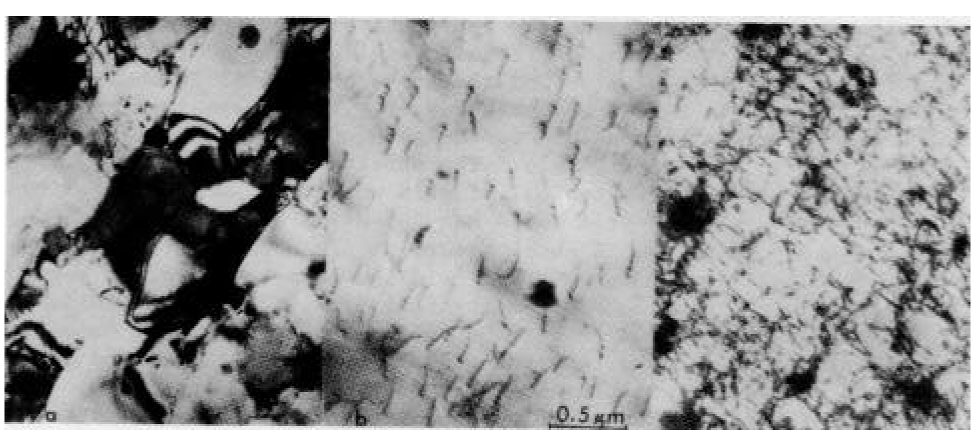

Laser shocking of weld zones has potential application in several areas of industry. A shock treatment could be beneficial wherever welded aluminum structures are used and the structure, or part, is designed to accommodate the mechanical properties of the weld. For example, in seam-welded aluminum pipe, a postweld laser shock treatment would increase the strength properties in the welded area and thus reduce the wall thickness required for safe operation. A laser shock process also may find application in welded rail structures or in the welded aluminum hulls of high-speed surface ships.

Another application area presently being investigated is the use of laser generated shocks to improve the fatigue properties of regions around fasteners in airplane structures. Tests conducted to date show large improvements in fatigue life are produced by the laser shock process. Both crack growth and fastened joint specimens in plate thicknesses up to 0.25 inches have been tested. For example, in a 7075 T6 aluminum alloy, the high cycle fatigue life of laser treated fastened joint specimens was approximately 100 times greater than untreated specimens and the rate of crack growth in laser treated crack growth specimens was reduced by an even greater factor.

STEEL ALLOYS

As noted earlier in this paper, the Fe 3wt% Si alloy was studied because it can be readily etch pitted to show the distribution and approximate magnitude of plastic deformation. The type of deformation generated in this alloy from laser shocking is shown in Figure 7. These transverse sections were taken from discs of different thicknesses which were laser shocked on the top surface. The darker regions correspond to areas which have undergone higher deformation than the lighter zones. As shown in Figure 7, the amount of deformation at the front and back surface was about the same. Also, the lightly deformed central layer decreased in thickness with decreasing specimen thickness. The thinner specimens showed shock induced deformation over most of the thickness. Uniform shock hardening corresponding to about 1 percent tensile strain was observed in the 0.02 cm thick specimen. Both slip and twinning were present in the shocked specimens.

In addition to the iron alloy, stainless steel also has been laser shocked. This material exhibits a cumulative improvement in material properties from repeated laser shocks., For example, the surface hardness of 304 SS showed little increase after one shock. As shown in Figure 8, five shocks were able to increase surface hardness by about 40 percent. This increase in hardness with multiple shocks can be attributed to an increase in dislocation density as shown by the transmission electron micrographs in Figure 9. The ability to multiple shock a material and improve properties in cumulative way is an important aspect of laser shock processing because multiple shocking with a laser is relatively straightforward. In this way, significant improvements in material properties can be realized at peak pressures too low to cause significant hardening with a single pulse.

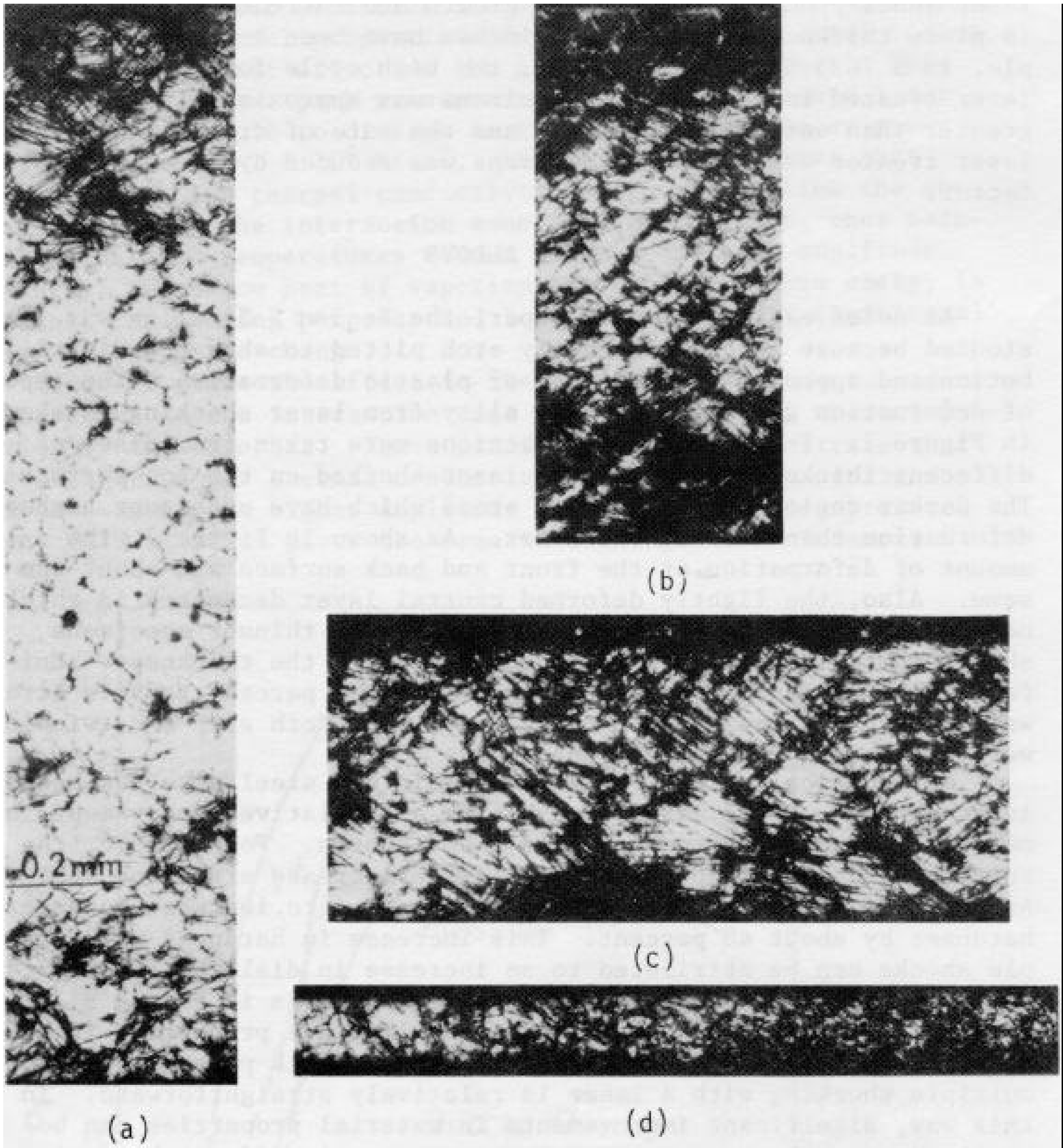

Fig. 7. Laser induced shock deformation in an Fe 3 wt% Si Alloy.
(a) t = 0.181 cm. (b) t = 0.093 cm.
(c) t = 0.051 cm. (d) t = 0.020 cm.

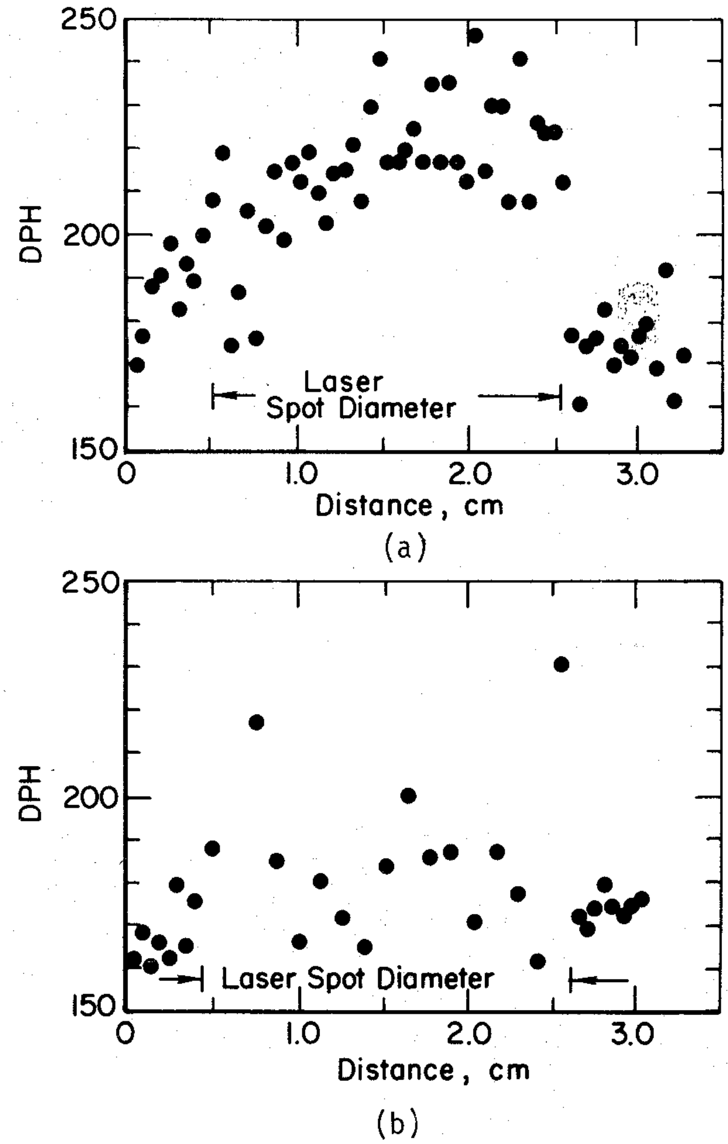

Fig. 8. Surface microhardness profiles across laser shocked regions after one and five successive shock of AISI 304. (a) One shock, pulse length, 22 nsec, peak pressure, 4.9 GPa. (b) Five Shocks, pulse length, 22 nsec, peak pressure, 4.9 GPa.

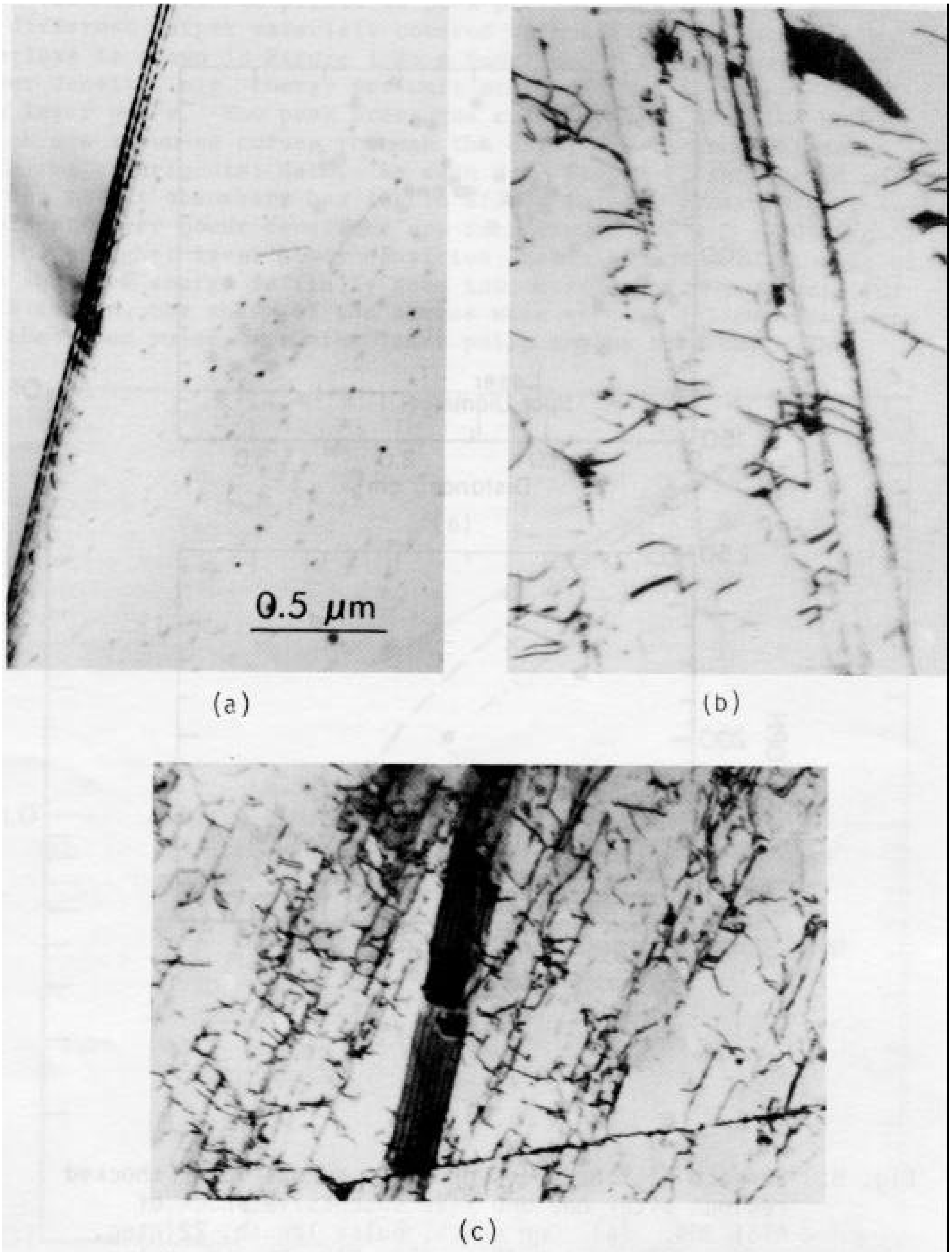

Fig. 9. Effect of multiple shocks on dislocation substructure in 304 stainless steel. The shocking conditions were black paint plus water overlay. 4.9 GPa peak pressure and a 22 nsec pulse duration. The specimens were shocked from one side only. (a) Unshocked. (b) One shock. (b) Five shocks.

TITANIUM ALLOYS

Titanium and titanium-vanadium alloys containing up to 20 wt percent vanadium were laser shocked. The titanium-vanadium alloys were selected to investigate the possibility of inducing an ω phase transformation by the laser generated pressure waves. Surface and bulk microhardness measurements showed hardness increases of up to 20 percent which were relatively independent of composition. There were modest increases in tensile strength in some of the alloys. The presence of a shock induced phase transformation was not detected in magnetic susceptibility measurements and examination by transmission electron micrographs. Effects of laser induced shock waves to these alloys are still under investigation.

CONCLUSIONS

It has been determined that pressures up to approximately 10 GPa can be generated in metals and alloys with short duration laser pulses. These pressures can be generated in an air or other gas environment if the surface is covered with a transparent material. The duration of the pressure waves, which is dictated by the laser energy deposition time, is typically less than a few tenths of a microsecond. These pressure environments are able to modify the microstructures and mechanical properties, e.g., strength, hardness, and fatigue, of several aluminum, iron, and titanium alloys. In all of the cases examined, the shock microstructures show the presence of tangled networks of dislocations which are similar in their appearance to high explosive and flyer plate shocked material.

ACKNOWLEDGEMENTS

The help of B. Campbell and M. Cantin in assisting with the laser experiments and material analyses is hereby acknowledged. R. Jung is also acknowledged for his assistance in the computer modeling. These studies were supported in part by the National Science Foundation, National Aeronautics and Space Administration, and the Army Research Office.

REFERENCES

1. G. A. Askar'yan and E. M. Moroz, JETP Lett. 16, 1638 (1963).
2. R. M. White, J. Appl. Phys. 34, 2123 (1963).
3. N. C. Anderholm, Appl. Phys. Lett. 16, 1133 (1970).
4, J. D. O'Keefe and C. H. Skeen, Appl. Phys. Lett. 21, 454 (1972).
5. J. A. Fox, Appl. Phys. Lett. 24, 461 (1974).
6. L. C. Yang, J. Appl. Phys. 45, 2601 (1974).
7. B. P. Fairand, A. H. Clauer, R. G.. Jung, and B. A. Wilcox, Appl. Phys. Lett. 25, 431 (1974).
8. B. P. Fairand and A. H. Clauer, Opt. Commun. 18, 488 (1976).
9. B. P. Fairand, B. A. Wilcox, W. J. Gallagher, and D. N. Williams, J. Appl. Phys. 43, 3893 (1972).
10. A. H. Clauer, B. P. Fairand, and B. A. Wilcox, Met. Trans. A 8A, 119 (1977).

11. A. H. Clauer, B. P. Fairand, and B. A. Wilcox, Met. Trans. A 8A, 1872 (1977).
12. J. D. O'Keefe, C. H. Skeen, and C. M. York, J. Appl. Phys. 44, 4622 (1973).
13. A. L. Stevens and O. E. Jones, J. Appl. Mech, 359 (June 1972).
14. B. P. Fairand and A. H. Clauer, J. Appl. Phys. (December 1978).
15. A. J. Jacobs, "Fundamental Aspects of Stress Corrosion Cracking", National Association of Corrosion Engineers, Houston, Texas, p. 530 (1969).
16. R. B. Herring and G. B. Olson, "The Effect of Aging Time on Spallation of 2024-T6 Aluminum," AMMRC TR41-61, Army Materials and Mechanics Research Center (December 1971).